

Profiling Novel Sulfonamide Antitumor Agents with Cell-based Phenotypic Screens and Array-based Gene Expression Analysis

Akira Yokoi, Junro Kuromitsu, Takatoshi Kawai, Takeshi Nagasu, Naoko Hata Sugi, Kentaro Yoshimatsu, Hiroshi Yoshino, and Takashi Owa¹

Laboratory of Seeds Finding Technology [A. Y., J. K., T. K., T. N., T. O.], Discovery Research Laboratories II [N. H. S., K. Y.], and Exploratory Research Laboratories [H. Y.], Eisai Co. Ltd., Ibaraki 300-2635, Japan

Abstract

A series of small molecules from sulfonamide-focused libraries have been evaluated in these laboratories to discover novel antitumor agents. Cell-based screens using flow cytometric analysis revealed the presence of two distinct classes of cell cycle inhibitors in this series; one (including E7010 and ER-67865) arrested mitosis by preventing tubulin polymerization; and the other (including E7070 and ER-68487) caused a decrease in the S-phase fraction along with cell cycle perturbation in G₁ and/or G₂ via an unknown mechanism(s). To further characterize both classes of antitumor sulfonamides with respect to their effects on gene expression, we used oligonucleotide microarray analysis for representative compounds. Consistent with the phenotypic observations, essentially the same transcription profiles were found between E7010 and ER-67865 and also between E7070 and ER-68487. However, there was very little overlap between genes affected by E7010 and E7070. As a characteristic expression change for microtubule-depolymerizing agents, the down-regulation of α -tubulin transcripts was evident in both E7010- and ER-67865-treated cells. On the other hand, E7070 and ER-68487 repressed significantly the expression of a variety of genes involved in metabolic processes, cell cycle progression, immune response, and signal transduction. Of the compounds examined, E7010 and E7070 have progressed to clinical trials, demonstrating some objective responses in the Phase I setting. Described herein is profiling of novel anticancer drug candidates from the sulfonamide class based on phenotypic screens and gene expression analysis. This includes a translational research that may suggest potentially useful markers for pharmacodynamic drug assessment in clinic.

Introduction

The advent of high-throughput screening systems has allowed us to evaluate a large number of small molecules in parallel and automated fashions. In response to this screening innovation, one of the greatest concerns in recent drug discovery programs has been directed toward how to design and prepare compound libraries for getting “hits” in various biological assays (1). In this regard, historical reviews of drug discovery often give us practical lessons. One highly informative example is represented by the sequential development of sulfonamide therapeutics such as antibiotic sulfa drugs, insulin-releasing hypoglycemic agents, carbonic anhydrase-inhibitory diuretics, high-ceiling diuretics, and antihypertensive drugs (2–4). These diverse pharmacological effects were serendipitously found through the serial derivatization of a single chemical structure of sulfanilamide, indicating that the sulfonamide motif is a crucial functionality capable of interacting with multiple cellular targets. Therefore, we have seriously considered that novel anticancer chemotherapeutics might be discovered from the sulfonamide class. In fact, our drug discovery efforts using sulfonamide-focused libraries have resulted in the finding of E7010 and E7070 as anticancer drug candidates (5–8).

E7010 was shown to reversibly bind to the colchicine site of β -tubulin, thereby halting mitosis (9). The compound exhibited good *in vivo* efficacy against rodent tumors and human tumor xenografts (10). As a p.o.-active antimitotic agent, E7010 demonstrated objective responses in 2 of 16 patients in the single-dose study of Phase I trials; spinal cord metastasis was reduced by 74% in a patient with uterine sarcoma, and a minor response was observed in a pulmonary adenocarcinoma patient (11). In contrast to E7010, E7070 was found to block cell cycle progression of P388 murine leukemia cells in the G₁ phase, accompanied by a decrease in the S-phase fraction (6). Although its precise mode of action has not yet been determined, E7070 appears to be considerably different from conventional anticancer drugs in clinical use with respect to its cell cycle effect and its tumor type selectivity (8, 12). Furthermore, preclinical animal tests established the promising efficacy of E7070 against human tumor xenografts (12). Thus, the compound has progressed to clinical evaluation in collaboration with the European Organization for Research and Treatment of Cancer (13). In the Phase I setting, one patient with a uterine adenocarcinoma experienced a partial response with a >50% shrinkage of measurable tumors after i.v. administration on the weekly schedule (14). Another partial response was reported in a patient with breast cancer on the daily \times 5 schedule (15). Phase II studies of E7070 are currently ongoing in Europe and the United States.

Received 9/18/01; revised 12/31/01; accepted 1/7/02.

¹ To whom requests for reprints should be addressed, at Laboratory of Seeds Finding Technology, Eisai Co., Ltd. 5-1-3 Tokodai, Tsukuba, Ibaraki 300-2635, Japan. Phone: 81-(0)298-47-5868; Fax: 81-(0)298-47-2037; E-mail: t-owa@hhc.eisai.co.jp.

On the basis of the significant observations described above, we decided to further examine E7010, E7070, and some other antitumor sulfonamides from these two classes of cell cycle inhibitors with special interest in their effects on gene expression. Array-based hybridization technology (16, 17) has enabled monitoring of the mRNA levels of thousands of genes simultaneously, displaying the patterns of transcriptional changes under various conditions. In particular, global gene expression analysis with a biologically active small molecule represents the chemical genomic approach to understanding complex cellular processes relevant to drug activity (18). An early example is a method for drug target validation with the immunosuppressants cyclosporin A and FK506 using yeast cDNA microarrays (19). In the report, the authors also highlighted the applicability of this technology to identifying secondary drug target effects using yeast mutant strains defective in drug target genes. A more recent microarray analysis disclosed that some nutrient-sensitive signal pathways were regulated by another immunosuppressive agent, rapamycin (20). In the Developmental Therapeutics Program of the National Cancer Institute, the correlation between gene expression and drug activity patterns in the NCI60 lines has been assessed to integrate large databases on gene expression and anticancer drug pharmacology (21). All of these reports, comprehensively illustrating genome-wide studies for rational drug discovery and development, urged us to use oligonucleotide microarray analysis for profiling the E7010 and E7070 classes of antitumor sulfonamides on the basis of compound-induced transcriptional changes. In the present study, several sulfonamide molecules containing the 2-oxindole or 3-cyanoindole core were evaluated together with E7010 and E7070 in cell-based screens, *i.e.*, the MTT² assay and FACS analysis. Furthermore, E7010, E7070, ER-67865, and ER-68487 (Fig. 1) were selected as representative compounds for array-based transcriptional profiling.

Materials and Methods

Chemical Synthesis of Sulfonamide Derivatives. The compounds listed in Tables 1 and 2 were synthesized using procedures published previously (5–7). E7010, E7070, and compounds **7**, **9** (ER-68487), and **10** were characterized by spectroscopic and analytical data as described previously (5, 6). The other new derivatives were characterized according to the following general methods. Melting points were determined on a Yanagimoto micromelting point apparatus and are reported uncorrected. Proton (¹H) NMR spectra were obtained at 400 MHz on a Varian UNITY 400 spectrometer in DMSO-*d*₆. Carbon (¹³C) NMR spectra were obtained at 150 MHz on a JEOL JNM- α 600 spectrometer in DMSO-*d*₆. Chemical shifts are expressed in δ (ppm) units relative to tetramethylsilane reference. Mass spectra (HRMS) were recorded on a JEOL JMS-SX102AAQQ using a direct intro-

² The abbreviations used are: MTT, 3-(4,5-dimethylthiazoyl-2-yl)-2,5-diphenyltetrazolium bromide; FACS, fluorescence-activated cell sorting; NMR, nuclear magnetic resonance; mp, melting point; RT-PCR, reverse transcription-PCR.

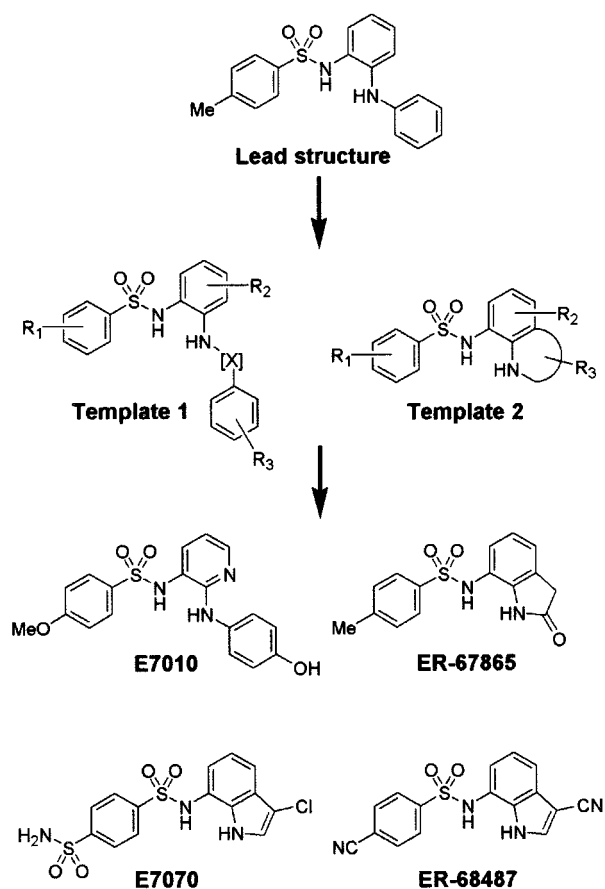


Fig. 1. Drug discovery flow chart of a series of antitumor sulfonamides.

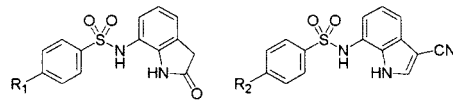
duction method in the EI⁺ ion mode. Elemental analyses (C, H, N) were carried out at the Eisai Analytical Chemistry Section, and the results were within $\pm 0.4\%$ of the theoretical values.

N-(1,3-Dihydro-2H-indol-2-on-7-yl)-4-methoxybenzenesulfonamide (1). mp 266–267°C. ¹H NMR (400 MHz, DMSO-*d*₆, δ): 3.46 (2H, s), 3.80 (3H, s), 6.81 (1H, dd, *J* = 8.2, 7.1 Hz), 6.89 (1H, dd, *J* = 8.2, 1.1 Hz), 6.97 (1H, dd, *J* = 7.1, 1.1 Hz), 7.02–7.07 (2H, AA'BB'), 7.62–7.67 (2H, AA'BB'), 9.37 (1H, br s), 9.82 (1H, s); ¹³C NMR (150 MHz, DMSO-*d*₆, δ): 35.81, 55.62, 114.29, 119.29, 121.51, 121.56, 121.97, 126.98, 129.04, 130.89, 137.00, 162.53, 175.53. HRMS (EI) M⁺ calculated for C₁₅H₁₄N₂O₄S 318.0675, found 318.0687. Analysis calculated for C₁₅H₁₄N₂O₄S: C 56.59, H 4.43, N 8.80; found: C 56.52, H 4.35, N 8.80.

N-(1,3-Dihydro-2H-indol-2-on-7-yl)-4-methylbenzenesulfonamide (2, ER-67865). mp 269–272°C. ¹H NMR (400 MHz, DMSO-*d*₆, δ): 2.34 (3H, s), 3.46 (2H, s), 6.80 (1H, dd, *J* = 8.2, 7.1 Hz), 6.87 (1H, dd, *J* = 8.2, 1.3 Hz), 6.98 (1H, dd, *J* = 7.1, 1.3 Hz), 7.30–7.37 (2H, AA'BB'), 7.58–7.63 (2H, AA'BB'), 9.43 (1H, s), 9.84 (1H, s); ¹³C NMR (150 MHz, DMSO-*d*₆, δ): 20.95, 35.82, 119.17, 121.52, 121.62, 121.96, 126.85, 127.02, 129.59, 136.51, 137.05, 143.39, 175.55. HRMS (EI) M⁺ calculated for C₁₅H₁₄N₂O₃S 302.0726, found 302.0721. Analysis calculated for C₁₅H₁₄N₂O₃S: C 59.59, H 4.67, N 9.27; found: C 59.76, H 4.71, N 9.16.

Table 1 Inhibition of cell proliferation (IC₅₀) for sulfonamide antitumor agents

The MTT assays were performed twice in triplicate with each test compound.



Compd	IC ₅₀ (μM) ^a					
	colon38	P388	HCT116-C9	HCT116-C9-C1 ^b	LX-1	LX-1-E2 ^b
1: R ₁ = -OCH ₃	0.79	0.35	0.57	0.60 (1.1)	0.47	1.1 (2.3)
2: R ₁ = -CH ₃ (ER-67865)	0.56	0.36	0.60	0.58 (0.97)	0.46	1.1 (2.4)
3: R ₁ = -NH ₂	5.9	3.9	3.6	3.8 (1.1)	3.3	5.1 (1.5)
4: R ₁ = -Cl	14	6.7	8.0	8.4 (1.1)	6.4	14 (2.2)
5: R ₁ = -SO ₂ NH ₂	>100	>100	>100	>100 (ND ^c)	>100	>100 (ND ^c)
6: R ₂ = -SO ₂ NH ₂	0.74	2.9	0.58	79 (1.4 × 10 ²)	1.1	21 (19)
7: R ₂ = -CONH ₂	2.0	7.3	1.5	>100 (>67)	1.9	33 (17)
8: R ₂ = -COCH ₃	0.74	2.7	0.53	56 (1.1 × 10 ²)	0.94	41 (44)
9: R ₂ = -CN (ER-68487)	0.37	1.6	0.34	43 (1.3 × 10 ²)	0.74	49 (66)
10: R ₂ = -OCH ₃	0.52	2.2	0.49	4.3 (8.8)	1.0	5.7 (5.7)
E7010	1.0	0.86	0.85	0.89 (1.0)	0.63	1.1 (1.7)
E7070	0.26	1.2	0.23	31 (1.3 × 10 ²)	0.73	24 (33)

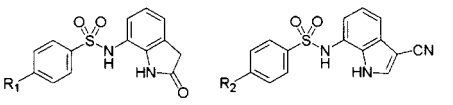
^a IC₅₀s were calculated using the least-squares method to afford the means of six independent data obtained from two separate assays. Errors were within ±10% of the reported values.

^b Resistance factors were calculated as IC₅₀s for the resistant cell line/IC₅₀s for the parental cell line.

^c ND, not determined.

Table 2 Effects of sulfonamide antitumor agents on cell cycle progression and tubulin polymerization

FACS analyses were performed three times using propidium iodide staining to quantitate the DNA content. Mitotic index represents the percentage of mitotic cells under a microscope. Assembly of microtubules was evaluated turbidimetrically at 350 nm 30 min after the reaction mixture was warmed from 4 to 37°C. The experiments were carried out three times with each test compound.



Compd	FACS analysis ^a		Inhibition of tubulin polymerization, IC ₅₀ (μM) ^e	
	P388	HCT116-C9	Mitotic index (%) ^d	
1: R ₁ = -OCH ₃	G2/M arrest	G2/M arrest	58%	2.1
2: R ₁ = -CH ₃ (ER-67865)	G2/M arrest	G2/M arrest	60%	2.5
3: R ₁ = -NH ₂	4C~8C ^b	4C~8C ^b	51%	8.9
4: R ₁ = -Cl	4C~8C ^b	4C~8C ^b	46%	19
5: R ₁ = -SO ₂ NH ₂	NC ^c	NC ^c	5.0%	>100
6: R ₂ = -SO ₂ NH ₂	G1 up and S down	G2/M up and S down	4.2%	>100
7: R ₂ = -CONH ₂	G1 up and S down	G2/M up and S down	4.5%	>100
8: R ₂ = -COCH ₃	G1 up and S down	G2/M up and S down	3.9%	>100
9: R ₂ = -CN (ER-68487)	G1 up and S down	G2/M up and S down	4.1%	>100
10: R ₂ = -OCH ₃	G2/M arrest	G2/M arrest	51%	9.2
E7010	G2/M arrest	G2/M arrest	55%	2.2
E7070	G1 up and S down	G2/M up and S down	3.9%	>100

^a Drug treatment at 8 μM for 12 h.

^b The appearance of tetraploid (8C) cells indicates that the cells went through an additional DNA replication without finishing mitosis.

^c NC, no change.

^d Drug treatment at 8 μM for 12 h. The mitotic index of control (nontreated) P388 cells measured 4.8%.

^e The maximum drug concentration was fixed at 100 μM. IC₅₀s were calculated using the least-squares method to afford the means of three independent experimental data. Errors were within ±10% of the reported values.

4-Amino-*N*-(1,3-dihydro-2*H*-indol-2-on-7-yl)benzenesulfonamide (3). mp 278–280°C. ¹H NMR (400 MHz, DMSO-*d*₆, δ): 3.45 (2H, s), 5.99 (2H, s), 6.48–6.54 (2H, AA'BB'), 6.81 (1H, dd, *J* = 8.2, 8.1 Hz), 6.94 (1H, dd, *J* = 8.1, 1.1 Hz), 6.96 (1H, dd, *J* = 8.2, 1.1 Hz), 7.32–7.37 (2H, AA'BB'), 9.06 (1H, s), 9.75 (1H, s); ¹³C NMR (150 MHz, DMSO-*d*₆, δ): 35.83, 112.53, 120.08, 120.92, 121.28, 121.47, 124.02, 126.78, 128.82, 136.11, 152.95, 175.54. HRMS (EI) M⁺ calculated for C₁₄H₁₃N₃O₃S 303.0679, found 303.0702. Analysis calculated for C₁₄H₁₃N₃O₃S: C 55.43, H 4.32, N 13.85; found: C 55.32, H 4.34, N 13.77.

4-Chloro-*N*-(1,3-dihydro-2*H*-indol-2-on-7-yl)benzenesulfonamide (4). mp 277–279°C. ¹H NMR (400 MHz, DMSO-*d*₆, δ): 3.47 (2H, s), 6.80 (1H, dd, *J* = 8.2, 1.6 Hz), 6.82 (1H, dd, *J* = 8.2, 6.4 Hz), 7.02 (1H, dd, *J* = 6.4, 1.6 Hz), 7.60–7.65 (2H, AA'BB'), 7.68–7.73 (2H, AA'BB'), 9.61 (1H, br s), 9.91 (1H, s); ¹³C NMR (150 MHz, DMSO-*d*₆, δ): 35.83, 118.54, 121.56, 122.20, 122.83, 127.18, 128.81, 129.32, 137.91, 138.00, 138.22, 175.59. HRMS (EI) M⁺ calculated for C₁₄H₁₁N₂O₃SCl 322.0180, found 322.0166. Analysis calculated for C₁₄H₁₁N₂O₃SCl: C 52.10, H 3.44, N 8.68; found: C 52.15, H 3.39, N 8.59.

***N*-(1,3-Dihydro-2*H*-indol-2-on-7-yl)-1,4-benzenedisulfonamide (5).** mp >300°C. ¹H NMR (400 MHz, DMSO-*d*₆, δ): 3.48 (2H, s), 6.79 (1H, dd, *J* = 8.2, 1.3 Hz), 6.82 (1H, dd, *J* = 8.2, 6.4 Hz), 7.02 (1H, dd, *J* = 6.4, 1.3 Hz), 7.60 (2H, s), 7.89–7.94 (2H, AA'BB'), 7.94–7.99 (2H, AA'BB'), 9.75 (1H, s), 10.02 (1H, s); ¹³C NMR (150 MHz, DMSO-*d*₆, δ): 35.87, 118.43, 121.57, 122.19, 122.49, 126.57, 127.28, 127.75, 137.92, 142.32, 147.75, 175.64. HRMS (EI) M⁺ calculated for C₁₄H₁₃N₃O₅S₂ 367.0298, found 367.0321. Analysis calculated for C₁₄H₁₃N₃O₅S₂: C 45.77, H 3.57, N 11.44; found: C 45.91, H 3.43, N 11.30.

***N*-(3-Cyano-1*H*-indol-7-yl)-1,4-benzenedisulfonamide (6).** mp 273–274°C. ¹H NMR (400 MHz, DMSO-*d*₆, δ): 6.73 (1H, d, *J* = 7.7 Hz), 7.08 (1H, dd, *J* = 8.0, 7.7 Hz), 7.46 (1H, d, *J* = 8.0 Hz), 7.59 (2H, s), 7.88–7.93 (2H, AA'BB'), 7.93–7.99 (2H, AA'BB'), 8.22 (1H, d, *J* = 3.1 Hz), 10.34 (1H, s), 11.98–12.06 (1H, m); ¹³C NMR (150 MHz, DMSO-*d*₆, δ): 84.92, 115.84, 116.61, 118.01, 121.97, 122.23, 126.56, 127.76, 128.50, 130.35, 134.93, 141.97, 147.77. HRMS (EI) M⁺ calculated for C₁₅H₁₂N₄O₄S₂ 376.0302, found 376.0309. Analysis calculated for C₁₅H₁₂N₄O₄S₂: C 47.86, H 3.21, N 14.88; found: C 47.90, H 3.12, N 14.89.

4-Acetyl-*N*-(3-cyano-1*H*-indol-7-yl)benzenesulfonamide (8). mp 258–259°C. ¹H NMR (400 MHz, DMSO-*d*₆, δ): 2.60 (3H, s), 6.74 (1H, d, *J* = 7.7 Hz), 7.05 (1H, dd, *J* = 7.9, 7.7 Hz), 7.42 (1H, d, *J* = 7.9 Hz), 7.81–7.88 (2H, AA'BB'), 8.03–8.10 (2H, AA'BB'), 8.21 (1H, s), 10.34 (1H, br s), 11.92–12.07 (1H, m); ¹³C NMR (150 MHz, DMSO-*d*₆, δ): 26.96, 84.88, 115.83, 116.49, 117.95, 121.98, 122.32, 127.25, 128.44, 128.90, 130.29, 134.89, 139.79, 142.79, 197.24. HRMS (EI) M⁺ calculated for C₁₇H₁₃N₃O₃S 339.0679, found 339.0668. Analysis calculated for C₁₇H₁₃N₃O₃S: C 60.17, H 3.86, N 12.38; found: C 60.08, H 3.96, N 12.27.

Cancer Cell Lines. Colon 38 murine adenocarcinoma, P388 murine leukemia, and LX-1 human small cell lung carcinoma were supplied by the Cancer Chemotherapy Center, Japan Foundation for Cancer Research (Tokyo, Japan).

HCT116 human colon carcinoma was purchased from American Type Culture Collection (Manassas, VA). HCT116-C9, an E7070-sensitive subclone, was isolated from the parental HCT116 cell line by using a limiting dilution method. Two E7070-resistant subclones, HCT116-C9-C1 and LX-1-E2, were obtained from viable colonies after continuous E7070 exposure with serial dose escalation. All of these cancer cells were cultured at 37°C in a humidified atmosphere of 5% CO₂ in RPMI 1640 containing 10% heat-inactivated fetal bovine serum, penicillin (100 units/ml), and streptomycin (100 μg/ml).

Cell Growth Inhibition Assay. Exponentially growing cells (1.25 × 10³ cells/well for P388, 2.5 × 10³ cells/well for colon 38, 3.0 × 10³ cells/well for HCT116-C9 and HCT116-C9-C1, and 3.5 × 10³ cells/well for LX-1 and LX-1-E2) were seeded into 96-well microtiter plates and precultured for 1 day. Each of the test compounds was dissolved at 20 mM in DMSO (22) and further diluted with the culture medium to prepare 3-fold serial dilutions with the maximum concentration being 100 μM after the addition into each well. The obtained dilutions were added to the plates, and then incubation was continued for an additional 3 days. The antiproliferative activity was measured by the MTT colorimetric assay (23).

Flow Cytometric Analysis. Exponentially growing cells (2.0 × 10⁵ cells/well for P388 and 4.5 × 10⁵ cells/well for HCT116-C9) were seeded in six-well plates and precultured for 1 day. Test compounds (2.0 mM solution in DMSO) were each added to the plates at the final concentration of 8 μM, and then incubation was continued for 12 or 24 h. For FACS analysis, the cells were fixed in 70% ethanol, treated with RNase (1 mg/ml), and stained with propidium iodide (50 μg/ml). The DNA content was quantified by detecting red fluorescence with a flow cytometer (FACSCalibur; Becton Dickinson), and analysis was done using CellQuest and Mod-Fit LT software (Becton Dickinson).

Mitotic Index. P388 cells (2.0 × 10⁵ cells/well in 24-well plates) were cultured with 8 μM of each test compound for 12 h. The cells were treated with 75 mM KCl, fixed with methanol and acetic acid (3:1), and stained with 0.1% crystal violet. The mitotic index was determined by counting at least 500 cells under a microscope.

Tubulin Polymerization Assay. Test compounds dissolved at graded concentrations in DMSO were each added to the wells of 96-well microtiter plates containing 1 mg/ml microtubule protein from bovine brain. A final DMSO concentration of 5% (v/v) and compound concentrations of 0.30, 1.0, 3.0, 10, 30, and 100 μM were used for assays in polymerization buffer [0.1 M 2-(*N*-morpholino)ethanesulfonic acid, 1 mM EGTA, and 0.5 mM MgCl₂, pH 6.8]. After 30-min incubation at 4°C, the mixture was warmed to 37°C with 1 mM GTP to start tubulin polymerization. Microtubule assembly was monitored by measuring the turbidity at 350 nm with a microplate reader (THERMO max; Molecular Devices) for 40 min kinetically. At the time point of 30 min, the polymerization of the control reached a plateau level. Therefore, the turbidity at 30 min was plotted on a linear scale versus the concentration of the test compound on a log scale, and

the drug concentration causing a 50% inhibition of polymerization was determined (6, 9).

High Density Oligonucleotide Array Expression Analysis. HCT116-C9 cells were plated at 5.0×10^6 cells/dish in 10-cm diameter dishes with 10 ml of fresh medium. After 24-h preincubation, the cells were treated for 12 h with $8 \mu\text{M}$ of each test compound or with 0.015% DMSO (as control). The following microarray experiments were all carried out in duplicate. Sample preparation was performed according to established protocols (17). In brief, total RNA was extracted from the cells using Trizol (Life Technologies, Inc.) and further purified with RNeasy columns (Qiagen). Double-stranded cDNA was prepared from 10 μg of total RNA using SuperScript Choice System (Life Technologies, Inc.) and T7-d(T)₂₄ primers. The cDNA product was purified by phenol/chloroform extraction. *In vitro* transcription was carried out with RNA Transcript Labeling kit containing biotinylated UTP and CTP (Enzo Diagnostics). After purification with RNeasy columns, the cRNA was fragmented and then hybridized to Affymetrix GeneChip HuGeneFL arrays. According to the EukGE-WS2 protocol, the probe arrays were washed and stained with streptavidin-phycoerythrin and biotinylated goat anti-streptavidin on an Affymetrix fluidics station. Fluorescence intensities were captured with a Hewlett Packard confocal laser scanner. All quantitative data were processed using the Affymetrix GeneChip software (17).

Real-Time RT-PCR Assay. The PCR-primers for selected genes were designed using the Primer Expression software (Perkin-Elmer Applied Biosystems) as follows: *glyceraldehyde-3-phosphate dehydrogenase*, 5'-GAAGGTGAAGGTCGGA-GTC-3' and 5'-GAAGATGGTGTATGGGATTTC-3'; *cyclin H*, 5'-GTCATTCTGCTGAGCTTGCACCTTA-3' and 5'-GAGAGAT-TCTACCAGGTCGTCATCA-3'; *basic transcription factor M_r 62,000 subunit (BTFp62)*, 5'-CCAAGTTACGAAGCTCTGTC-CAT-3' and 5'-TGTTAGGCTGTCTGGAGCATCTCT-3'; *CDC16*, 5'-TGTTGATTCTCAGAACGCATC-3' and 5'-TGTATCATCT-CGCCTAAGACCAAG-3'; *replication factor C M_r 37,000 subunit (RFC4)*, 5'-CAAAGCGCTACTCGATTAACAGGT-3' and 5'-CCTTGACCACAGCTTCTAGTTTGTGTC-3'; *proliferating cell nuclear antigen (PCNA)*, 5'-TTGCACGTATATGCCGAGATCT-3' and 5'-AACAGCTTCTCTCTTTATCGAC-3'; *mitotic centromere-associated kinesin (MCAK)*, 5'-ATCTCACCGAG-GCATAAGCTCCT-3' and 5'-ACAGTTCTCTCTTCTGAT-3'; γ -*tubulin*, 5'-CTCAAGAGGCTGACGCAGAAT-3' and 5'-CTGGCTGACATGATGGTAGACAC-3'. The SYBR Green assay was performed according to a two-step procedure. In the first step, 1 μg of total RNA from drug-treated cells was converted to cDNA through a reverse transcription step for 30 min at 48°C with TaqMan Reverse Transcription Reagents (Perkin-Elmer Applied Biosystems). In the second step, the PCR reaction with 4 ng of the cDNA product was carried out using SYBR Green PCR Core Reagents (Perkin-Elmer Applied Biosystems). Thermal cycling conditions were for 2 min at 50°C, for 10 min at 95°C followed by 40 cycles of 20 s at 95°C, for 20 s at 55°C, and then for 30 s at 72°C. The mRNA levels were monitored in real-time with the ABI PRISM 7700 sequence detection system (Perkin-Elmer Applied Biosystems).

Results

Antitumor Screens Using Growth Inhibition Assay, Cell Cycle Analysis, and Tubulin Polymerization Assay. Several sulfonamide compounds from our focused libraries were initially screened for the *in vitro* antiproliferative activity against colon 38, P388, HCT116-C9, HCT116-C9-C1, LX-1, and LX-1-E2. Drug concentrations required for 50% cell growth inhibition (IC₅₀s), listed in Table 1, were determined according to the 3-day MTT assay protocol (23). Further phenotypic characterizations of the test compounds were performed using cell cycle analysis and tubulin polymerization assay. The results are summarized in Table 2.

In the 2-oxindole-containing series, compounds **1-4** showed a pattern of antiproliferative activity similar to that of E7010; to all of these drugs: (a) P388 cells were somewhat more sensitive than colon 38; and (b) two E7070-resistant clones HCT116-C9-C1 and LX-1-E2 were not significantly cross-resistant. Antimitotic action of these compounds was confirmed severally by a G₂-M arrest phenotype in FACS analysis, a clear increase in the mitotic index, and a potent inhibition of microtubule assembly. A good correlation was found between potencies of each compound in growth inhibition assay and in tubulin polymerization assay, with a rank order of E7010 \approx **1** \approx **2** (ER-67865) $>$ **3** $>$ **4**. However, compound **5**, possessing an electron-withdrawing sulfamoyl (SO₂NH₂) group as the R₁ substituent similar to E7070, proved to be completely inactive: (a) both IC₅₀s for cell growth and tubulin polymerization were $>100 \mu\text{M}$; and (b) no increase in the mitotic index was observed in drug-treated cells as compared with control cells. These results suggest that an electron-donating group such as methoxy (CH₃O) or methyl (CH₃) at the position of R₁ is critical for the E7010 type of antiproliferative and antitubulin activities. From the complete loss of antitumor properties in compound **5**, it can be concluded that the 2-oxindole motif is unfit for interacting with a putative molecular target(s) of the E7070 class of compounds.

Compounds **6-9** in the 3-cyanoindole-containing series were comparable with E7070 with respect to: (a) preferential activity against colon 38 rather than P388; (b) marked cross-resistance of HCT116-C9-C1 and LX-1-E2 to all of these drugs; (c) cell cycle effect of G₁ or G₂-M increase coincident with S decrease; and (d) substantially no influence on mitotic index and tubulin polymerization. Of these, compound **9** (ER-68487) displayed an almost equal activity profile to that of E7070 in all of the antitumor screens used here. Although compound **10** also possesses the 3-cyanoindole core, its activity profile distinctly differed from those of the others in the same series: (a) the two E7070-resistant cell lines were less cross-resistant to compound **10** as compared with compounds **6-9** and E7070; and (b) its antimitotic action was evident from the results of FACS analysis, mitotic index measurement, and tubulin polymerization assay as shown in Table 2. Hence, it can be stated that the structure of *N*-(3-cyano-7-indolyl)benzenesulfonamide is adaptable to both activity types of E7010 and E7070, depending on the R₂ substituent. In other words, activity profiles of this series of compounds appear to be determined by the nature of the R₂ substituent rather than the framework.

Table 3 Transcriptional changes caused by sulfonamide antitumor agents

cRNA probes were prepared from drug-treated (at 8 μM for 12 h) and control HCT116-C9 cells. Up- and down-regulated genes were selected based on the following criteria of the Affymetrix software algorithm: (a) fold change, 3-fold or more alteration with at least one of the four test compounds; (b) differential call, I (increase) or D (decrease); (c) absence call, genes except for indicating A (absent) in both control and drug-treated cells; (d) genes satisfying all of (a)–(c) in the data set either before or after antibody amplification; (e) gene satisfying all of (a)–(d) in both data sets taken in duplicate. Fold change values for each test compound are presented. NC means “no change” for genes with <2-fold alteration.

■ : Up- or down-regulation at least 3-fold

■ : Up- or down-regulation at least 2-fold and less than 3-fold

(A) Up-regulated genes

Clone #	Gene Name	E7010	67865	68487	E7070	Function
U27193	Dual-specificity protein phosphatase 8	4.4	6.1	NC	NC	Cell signaling
U62015	Cyr61	4.1	3.9	NC	NC	ECM signaling, adhesion
M27436	Tissue factor gene, Alu repeat	4.0	3.5	NC	NC	ECM signaling, coagulation
J04111	c-Jun	6.2	4.5	NC	NC	Transcription, immediate-early response
X16707	Fra-1	7.2	4.7	NC	NC	Transcription, immediate-early response
U16306	Chondroitin sulfate proteoglycan 2	3.4	2.0	NC	NC	ECM component
Z18951	Caveolin	2.9	2.8	3.0	3.2	Scaffolding, membrane trafficking
J04152	Tumor-associated antigen GA733-1, M1S1	2.8	3.0	3.7	2.6	Unknown
HG3484-HT3678	Cdc-like kinase 1 (Clk1)	NC	NC	3.2	2.6	Cell cycle
S61953	c-ErbB3 receptor tyrosine kinase	NC	NC	3.4	3.1	Cell signaling

(B) Down-regulated genes

Clone #	Gene Name	E7010	67865	68487	E7070	Function
M97796	Id-2	-2.6	-3.1	NC	NC	Transcription
U00115	Zinc-finger protein bcl-6, B-cell lymphoma 6	-4.1	-3.2	NC	NC	Transcription
HG2259-HT2348	Tubulin, alpha 1	-9.7	-7.5	NC	NC	Cytoskeleton
X01703	Alpha-tubulin (b alpha 1)	-3.1	-3.4	NC	NC	Cytoskeleton
D14838	FGF-9	-4.4	-3.3	NC	NC	Growth factor
U59321	DEAD-box protein p72	-4.0	-2.1	NC	NC	ATP-dependent RNA helicase
M55905	Mitochondrial NAD(P)+ dependent malic enzyme	NC	NC	-5.6	-3.0	Metabolism, malate
U60808	CDP-diacylglycerol synthase	NC	NC	-3.1	-4.3	Metabolism, lipid
Y08682	Carnitine palmitoyltransferase I type I	NC	NC	NC	-3.4	Metabolism, lipid
J04501	Muscle glycogen synthase	NC	NC	-4.0	-3.5	Metabolism, carbohydrate
X51956	Neuron specific gamma enolase (NSE)	NC	NC	-3.0	-3.2	Metabolism, carbohydrate
U80034	Mitochondrial intermediate peptidase precursor	NC	NC	-2.3	-5.7	Metabolism, mitochondrial iron uptake
U89606	Pyridoxal kinase	NC	NC	-3.4	-5.4	Metabolism, vitamin B6
U22233	Methylthioadenosine phosphorylase	NC	NC	NC	-3.2	Metabolism, nucleotide/amino acid
U30313	Diadenosine tetraphosphatase	NC	NC	-2.2	-3.1	Metabolism, nucleotide
U34683	Glutathione synthetase	NC	NC	-2.2	-3.1	Metabolism, redox
L07540	Replication factor C (RFC) 36-kD subunit	NC	NC	-3.4	-3.9	Cell cycle, replication
U27459	Origin recognition complex protein 2 (ORC2) homolog	NC	NC	-3.3	-3.2	Cell cycle, replication
X06745	DNA polymerase alpha-subunit	NC	NC	-4.9	-4.0	Cell cycle, replication
J04088	DNA topoisomerase II (Topo II)	NC	NC	-2.6	-3.0	Cell cycle, replication, DNA repair
M95809	Basic transcription factor 62kD subunit (BTFp62)	NC	NC	-3.0	-4.2	Cell cycle, transcription, NER, TFIIH
U11791	Cyclin H	NC	NC	-8.5	-5.1	Cell cycle, TFIIH
L41870	Retinoblastoma susceptibility protein (RB1)	NC	NC	-3.0	-3.1	Cell cycle, tumor suppressor
U18291	CDC16	NC	NC	-3.5	-3.5	Cell cycle, protein turnover (APC/C), mitosis
U50939	Amyloid precursor protein-binding protein 1 (APP-BP1)	NC	NC	-4.3	-3.4	Cell cycle, protein turnover (Rub1/Nedd8)
D86981	Amyloid precursor protein-binding protein 2 (APP-BP2)	NC	NC	-2.8	-5.9	Unknown
M59911	Integrin alpha 3	NC	NC	-3.5	-2.6	Cell signaling, adhesion
X53587	Integrin beta 4	NC	NC	-2.8	-4.2	Cell signaling, adhesion
M29550	Calcineurin A1	NC	NC	-5.1	-2.5	Cell signaling
U18934	Receptor tyrosine kinase DTK	NC	NC	-2.6	-4.0	Cell signaling, hematopoiesis, adhesion
U81554	CaM kinase II isoform	NC	NC	-4.6	-5.3	Cell signaling
Z17227	Transmembrane receptor CRF2-4	NC	NC	-3.2	-3.9	IL-10 signaling, immune response
M97935	Transcription factor ISGF-3	NC	NC	-2.9	-3.1	IFN signaling, immune response, transcription
L25444	TAFII70-alpha	NC	NC	-2.0	-4.0	Transcription
U15306	DNA-binding protein NFX1	NC	NC	-4.8	-4.1	Transcription
U28963	Gps2	NC	NC	-4.2	-3.8	Transcription
D32002	Nuclear cap binding protein 1 (CBP80)	NC	NC	-8.4	-8.5	mRNA processing
M85085	Cleavage stimulation factor	NC	NC	-3.3	-5.0	mRNA processing
U30828	Splicing factor SRp55-2 (SRp55)	NC	NC	-2.1	-3.0	mRNA processing
U97188	Putative RNA binding protein KOC	NC	NC	-4.1	-2.7	mRNA processing
M93056	Monocyte/neutrophil elastase inhibitor	NC	NC	-4.5	-4.0	Immune response, inflammatory

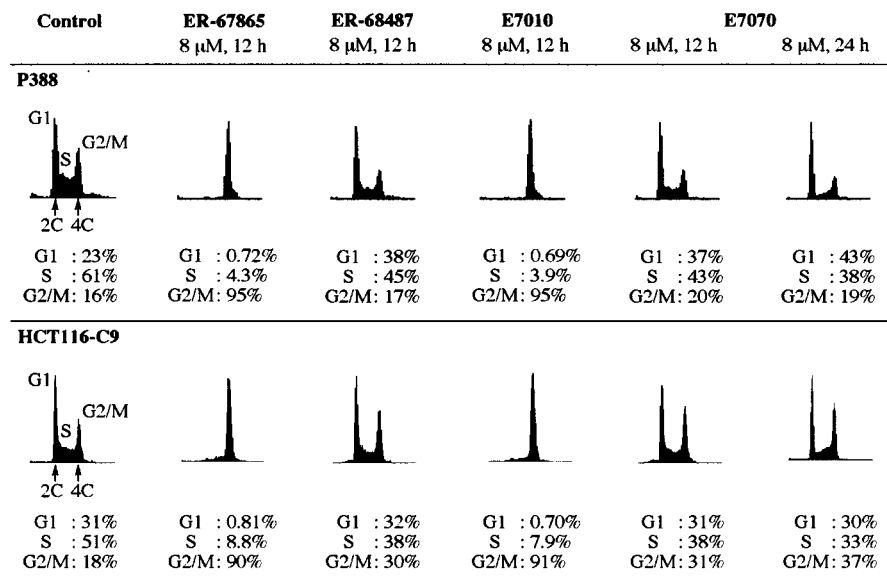
Table 3 Continued

U28831	Immuno-reactive with anti-PTH Ab	NC	NC	-3.4	-4.0	Immune response
Z68747	Imogen 38	NC	NC	-3.6	-3.3	Immune response, type I diabetes
D50663	Dynein (TCTEL1)	NC	NC	-3.7	-2.8	Cytoskeleton
M19267	Tropomyosin	NC	NC	-3.5	-4.2	Cytoskeleton
M62994	Filamin B	NC	NC	-2.8	-3.1	Cytoskeleton
U23028	Eukaryotic initiation factor 2B-epsilon (eIF2Br)	NC	NC	-3.4	-5.0	Translation
L07597	Ribosomal protein S6 kinase 2	NC	NC	-3.2	-3.5	Translation
U26648	Syntaxin 5A	NC	NC	-2.8	-4.4	Membrane trafficking
X70476	Subunit of coatomer complex	NC	NC	-2.8	-3.0	Membrane trafficking
M88163	Global transcription activator (hSNF2/SWI2)	NC	NC	-3.2	-2.0	chromatin remodeling
U61145	Enhancer of zeste homolog 2	NC	NC	-3.3	-2.6	chromatin modulation
S78085	PDCD2, Rp8 homolog	NC	NC	-10.4	-10.8	Apoptosis-related
X75535	PxF	NC	NC	-3.1	-4.0	Peroxisomal assembly
AF008445	Phospholipid scramblase 1	NC	NC	-9.6	-8.7	Plasma membrane remodeling
U23946	LUCA15	NC	NC	-3.1	-2.4	Putative tumor suppressor
AC002045	CIT987SK-A-589H1	NC	NC	-3.1	-2.2	Unknown
D14659	KIAA0103	NC	NC	-2.9	-5.4	Unknown
D29677	KIAA0054	NC	NC	NC	-3.0	Unknown
D29810	Unknown product	NC	NC	-3.3	-3.8	Unknown
D38552	KIAA0073	NC	NC	-3.7	-3.8	Unknown
D38553	KIAA0074	NC	NC	-3.8	-3.9	Unknown
D43947	KIAA0100	NC	NC	-3.0	-3.9	Unknown
D63875	KIAA0155	NC	NC	-3.0	-3.1	Unknown
D63880	KIAA0159	NC	NC	-2.9	-3.9	Unknown
D79988	KIAA0166	NC	NC	-2.2	-3.0	Unknown
D83781	KIAA0197	NC	NC	-4.3	-5.0	Unknown
D87446	KIAA0257	NC	NC	-4.5	-4.4	Unknown
S72904	APK1 antigen=MAB KI recognized	NC	NC	-3.3	-3.6	Unknown
U30521	P311 HUM -3.1	NC	NC	-3.4	-3.3	Unknown
U72515	C3f	NC	NC	-4.6	-3.4	Unknown
U79241	Clone 23759	NC	NC	-4.6	-11.3	Unknown

Drug Effects on Cell Cycle Progression. The cell cycle effects of representative antitumor sulfonamides (at 8 μ M) are illustrated in Fig. 2, based on FACS analyses using P388 and HCT116-C9 cell lines. A clear G₂-M arrest pattern was observed in both P388 and HCT116-C9 exposed to each of

E7010 and ER-67865 for 12 h. Judging from a significant increase in the mitotic index as shown in Table 2, this cellular phenotype may be mainly attributed to mitotic arrest. On the other hand, E7070 and ER-68487 caused a decrease in the S fraction to both cell lines after 12 h of treatment, accom-

Fig. 2. Flow cytometric analysis of sulfonamide antitumor agents. Drug effects on cell cycle progression of P388 and HCT116-C9 cells were examined according to the procedure described in "Materials and Methods." The experiments were performed three times with each test compound, and representative DNA histograms are presented. The percentages of the cells in each cell cycle phase were calculated using the ModFit LT software for the FACSCalibur flow cytometer (Becton Dickinson) to afford the means of three independent data.



panied by G₁ increase in P388 or G₂-M increase in HCT116-C9. The observations at the 24-h time point indicated a time-dependent manner of the cell cycle effect of E7070 (Fig. 2) or ER-68487 (data not shown). At this extended time point, inhibition of the G₁-S transition in HCT116-C9 was also evident from a marked drop in the early S fraction despite very few variations in G₁ proportion. There was no increase in the mitotic index after 12 h of treatment with E7070 or ER-68487, suggesting that the drug-induced G₂-M accumulation is attributable to cell cycle perturbation in the G₂ phase but not in the M phase. Furthermore, none of these four sulfonamides exhibited potent cell-killing activity up to the 12-h time point, indicated by the fact that the sub-G₁ fraction representing cells with fragmented DNA was not observed in the FACS analyses (24, 25). This supported that any drug treatment at 8 μ M for 12 h should permit us to detect earlier characteristic changes in gene expression before terminal cellular events such as apoptosis. The same experimental conditions were therefore used for the subsequent transcriptional profiling with oligonucleotide microarrays.

Array-based Transcriptional Profiling. To assess transcriptional effects of these four antitumor sulfonamides, gene expression analysis was performed with HuGeneFL arrays containing ~5600 gene probes. cRNA probes were prepared from drug-treated and control HCT116-C9 cells. The experimental conditions of drug treatment (at 8 μ M for 12 h) were rationalized by the FACS data. In addition, time course array experiments showed that the 12-h treatment produced more informative data for transcriptional profiling rather than the 3- or 6-h treatment (data not shown). Table 3 summarizes gene expression changes caused by each test compound, presenting fold change values of affected transcripts. The criteria for gene selection are described in the Table 3 legend.

E7010 treatment led to the 3-fold or more up-regulation and down-regulation of six and five genes, respectively. These include subsets of genes involved in immediate-early response (induction of *c-Jun* and *Fra-1*), extracellular matrix signaling (induction of *Cyr61* and *tissue factor gene*), and cytoskeletal organization (repression of two subtypes of α -*tubulin*). ER-67865 proved to be comparable with E7010 with respect to the fingerprint pattern of transcriptional changes as well as the above-mentioned activity profile, based on several antitumor screens. Despite their clear mitotic arrest phenotype, both compounds did not change significantly the expression of any cell cycle-regulatory gene at the 12-h time point.

E7070 altered at least 3-fold the levels of 60 transcripts; 58 of these were down-regulated, and the remaining 2 were up-regulated. This predominant transcriptional repression appears to be one of the characteristics for the array-based E7070 profile. These down-regulated genes can be classified into several categories according to their putative functions; cellular metabolism (10 genes), cell cycle regulation (9 genes), immune response (5 genes), cell signaling (5 genes), transcription (4 genes), mRNA processing (3 genes), cytoskeletal organization (2 genes), translation (2 genes), membrane trafficking (2 genes), and others. Some genes are counted for more than one category, e.g., *ISGF-3* is consid-

ered as participating in IFN-related cell signaling, immune response, and transcription (26). Also, there are subsets of genes involved in energy production (*mitochondrial malic enzyme*, *NSE*, *mitochondrial intermediate peptidase precursor*, and others), DNA replication (*RFC M_r 36,000 subunit*, *ORC2 homologue*, *DNA polymerase α -subunit*, and *Topo II*), the basic transcription factor TFIIH (*BTFp62* and *cyclin H*), protein turnover (*CDC16* and *APP-BP1*), and cell adhesion (*integrin β 4* and *receptor tyrosine kinase DTK*).

ER-68487 displayed a quite similar transcription profile to that of E7070. The compound up-regulated 4 genes and down-regulated 47 genes at least 3-fold. Of the total 51 genes, 41 are shared with E7070 on the same selection criteria. The overlap between the E7070 and ER-68487 profiles is more significant in case the 2-fold alteration is used as the threshold for gene selection. However, there is very little overlap between the profiles of E7010 class and E7070 class. Taken altogether, cell-based phenotypic profiling and array-based transcriptional profiling led to the same classification of these antitumor sulfonamides. Our array data well confirmed that compounds in the E7070 class operate by a completely different mechanism(s) of action from the E7010 type of antimitotic action.

Verification of Microarray Data by Quantitative RT-PCR. To verify the transcriptional changes detected by our microarray analysis, the quantitative RT-PCR technique was used. We were particularly interested in E7070-responsive genes because of a primary molecular target(s) for the compound being still unclear. Hence, the following seven cell cycle-related genes were selected for the verification: *cyclin H* and *BTFp62* involved in cell cycle coordination; *RFC4* and *PCNA* in DNA replication; *MCAK*, γ -*tubulin*, and *CDC16* (27) in mitosis. As shown in Fig. 3A, the RT-PCR data for HCT116-C9 cells were well consistent with the array data. At the 12-h time point, for example, the cyclin H transcript was down-regulated 5-fold by 8 μ M E7070 in microarray analysis, corresponding to the 5.9-fold down-regulation in PCR-based quantitation. As for *cyclin H*, *BTFp62*, and *CDC16*, all of which were down-regulated more than 3-fold, we further monitored the time course of their expression changes with the drug-sensitive and -resistant cell lines: HCT116-C9 and HCT116-C9-C1; LX-1 and LX-1-E2, respectively. The degree of transcriptional changes in these four cell lines showed a clear tendency to correlate with the rank order of drug sensitivity, HCT116-C9 > LX-1 > LX-1-E2 > HCT116-C9-C1 (Fig. 3B and Table 1). In the most resistant cell line HCT116-C9-C1, none of the three genes were down-regulated at all by 8 μ M E7070 during the time course tested. Although the E7070 treatment repressed about 2-fold the expression of *cyclin H* in another resistant clone LX-1-E2, this might be explained by the fact that the exposure of 8 μ M E7070 was not "cytotoxic" but somewhat "cytostatic" to this clone in the growth inhibition assay (data not shown).

Discussion

In this study, we used oligonucleotide microarrays containing probes of ~5600 human genes to investigate transcriptional effects of a series of sulfonamide antitumor agents. The expression profiling with thousands of genes illuminated a fingerprint pattern for each of four test com-

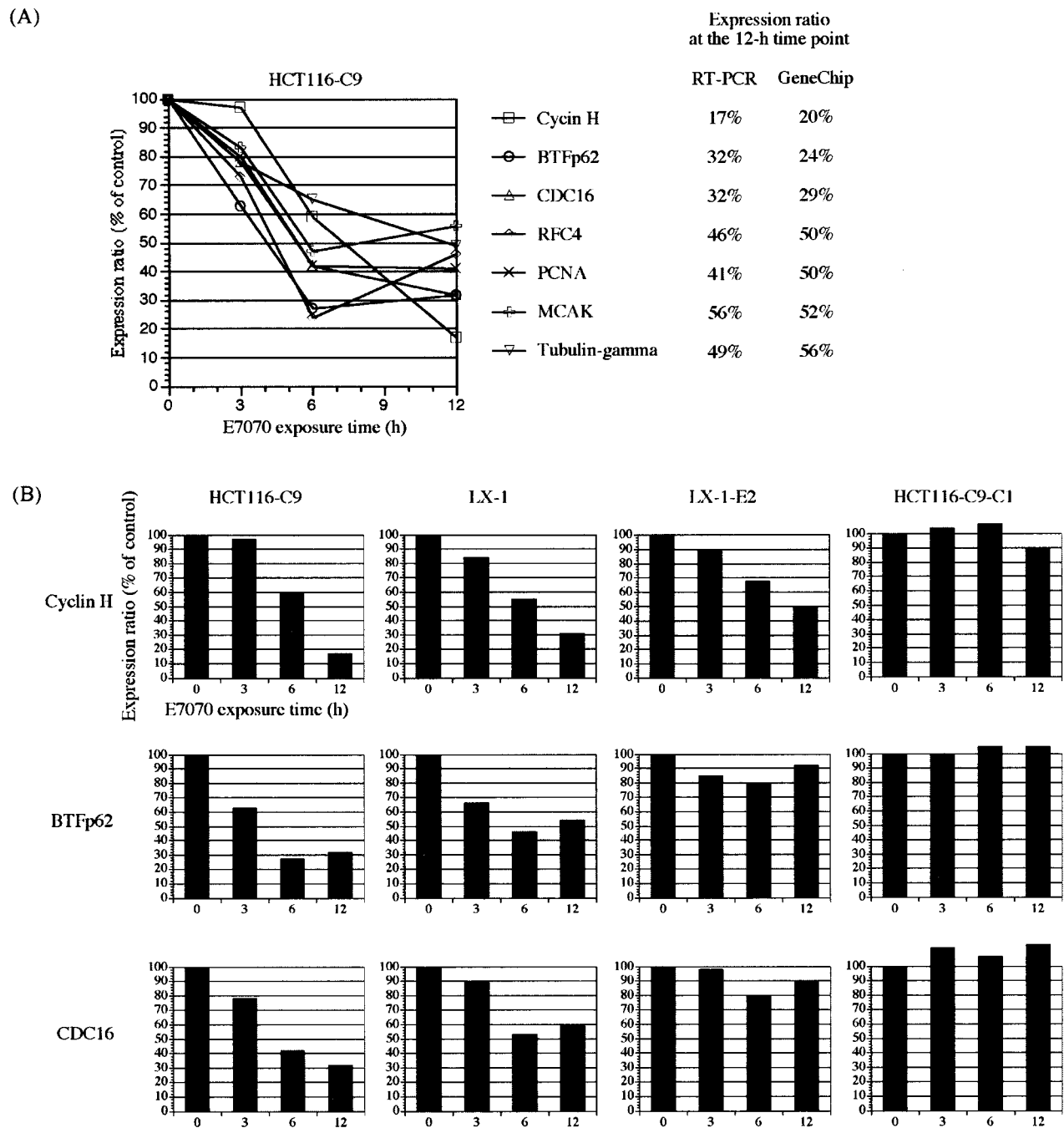


Fig. 3. Monitoring transcriptional changes of E7070-treated cancer cell lines using real-time RT-PCR. Four cell lines, HCT116-C9, HCT116-C9-C1, LX-1, and LX-1-E2, were treated with 8 μ M E7070. At time points of 3, 6, and 12 h, total RNA was extracted from each of these cells. For relative quantitation, the expression levels of the test genes were measured by real-time RT-PCR and normalized based on the *glyceraldehyde-3-phosphate dehydrogenase* levels as control.

pounds. Of these, E7010 and ER-67865 are mitotic arrest agents that disrupt microtubule assembly. The microarray analysis of another microtubule-depolymerizing agent, myoseverin, has been reported recently by Rosania *et al.* (28). A comparison between array-based fingerprints for myoseverin and the E7010 class of antimitotic sulfonamides indicates that the repression of *tubulin* transcripts

is in common despite their entirely different chemical structures. In our data, E7010 and ER-67865 repressed >3-fold the mRNA levels of two subtypes of α -*tubulin*, whereas myoseverin was shown to down-regulate the expression of two subtypes of β -*tubulin* 2- and 2.6-fold, respectively. The decrease in the expression levels of *tubulin* genes is known to be caused by a feedback reg-

ulatory mechanism resulting from the accumulation of tubulin monomers (29). Therefore, the *tubulin* down-regulation can be considered as a characteristic expression change with microtubule-depolymerizing agents, potentially usable as an end point indicative of drug efficacy in clinic.

Our results in cell-based phenotypic screens suggest that E7070 and ER-68487 belong to a novel class of cell cycle inhibitors. The FACS analyses revealed that both compounds reduced the proportion of S-phase and accumulated P388 cells in G₁ or HCT116-C9 cells in G₂-M. In the time course experiment with HCT116-C9, they were also found to inhibit G₁-S transition at the 24-h time point. The expression changes in several genes of HCT116-C9 appear to be consistent with these cellular phenotypes. E7070 and ER-68487 down-regulated >3-fold the expression of critical genes for DNA replication and mitosis, including *RFC M_r 36,000 subunit*, *ORC2 homologue*, *DNA polymerase α -subunit*, *CDC16*, and *APP-BP1* (associated with the S-M checkpoint; Ref. 30). These changes are thought to be linked with the drug-induced S decrease and G₂-M increase, although it has yet to be elucidated whether they are causes or effects of the phenotypic alterations.

As for the cell cycle perturbation, repression of the *cyclin H* transcript should be also noted. Western blotting analysis has further revealed that the expression of the cyclin H protein in HCT116-C9 is reduced by ~55% after 24 h of treatment with 8 μ M E7070.³ Cyclin H is known to form part of the CDK-activating kinase (CAK) together with CDK7 and MAT1 (31). CAK is not only a TFIID subcomponent that phosphorylates the COOH-terminal domain of the large subunit of RNA polymerase II (pol II) but also exists as a free complex to phosphorylate several cyclin-dependent kinases (CDKs) for their activation (32, 33). This activation at appropriate time points is essential for well-regulated cell cycling. Judging from the important role of cyclin H in coordinating the cell cycle, its repression at both mRNA and protein levels is likely to result in cell cycle arrest at several checkpoints. The fact that E7070 and ER-68487 simultaneously down-regulate the mRNA expression of another TFIID component BTFp62 indicates that the efficiency of transcription and nucleotide excision DNA repair might be suppressed as well by this class of antitumor agents (34).

In current clinical trials, there are a variety of anticancer drug candidates with novel mechanisms of action targeting angiogenesis, oncogenic signaling, cell cycle-regulatory machinery, and others. These agents may require different end points from those used traditionally for clinical drug assessment. In the well-defined classical design, the end point of Phase I trials is toxicity, whereas the end point of Phase II is response rate based on tumor regression. However, this design needs to be modified to properly evaluate novel agents that are expected to cause tumor growth suppression but not to reduce tumor size (35). Actually, E7070 was reported to produce many cases of "stable disease (SD)" in the Phase I studies (13–15, 22).

³ A.Yokoi and T. Owa, unpublished data.

A crucially important point for the development of these agents is considered to be the ability to assess the drug effect on their individual targets or pathways, providing validity and rationale for drug development. In this regards, DNA microarray technology appears to be particularly useful for detecting tumor changes in relevant genes to drug efficacy.

Of the genes affected by E7070 treatment in microarray analysis, we selected seven genes involved in cell cycle events for monitoring their mRNA levels by using real-time RT-PCR. Among them, *cyclin H* was most clearly down-regulated at a time point of 12 h in two E7070-sensitive cell lines HCT116-C9 and LX-1. The extent of the down-regulation was not only in a time-dependent manner but also in accord with the rank order of drug sensitivity of each cell line (HCT116-C9 > LX-1 > LX-1-E2 > HCT116-C9-C1), suggesting that a putative molecular mechanism of E7070 action has a close connection with the *cyclin H* transcription. Although the expression of *cyclin H* is known not to fluctuate through the cell cycle, its transcriptional regulation remains to be fully understood. A target finding study of E7070 may provide a new insight into the control mechanism of the *cyclin H* transcription, bringing us closer to using its expression change for the pharmacodynamic evaluation of E7070 efficacy.

In addition to the cell cycle-targeted effects, metabolic perturbation and immunomodulation were also conspicuous in the array data for the E7070 class of antitumor agents. Metabolic processes such as energy production are often accelerated in various cancers to maintain their abnormally aggressive proliferation. Cell adhesion and cytokine signaling are associated with formation and progress of some hyperproliferative diseases besides their pivotal roles in immune response. Therefore, it is likely that a wide range of the down-regulation of these genes may exert a fatal influence on the viability of cancer cells.

Our microarray data showed that both of E7070 and ER-68487 down-regulated three genes rather strongly (over 8-fold); *nuclear cap binding protein 1 (CBP80)*, *PDCD2* (an Rps8 homologue), and *phospholipid scramblase 1*:

(a) CBP80 forms the heterodimeric nuclear cap-binding complex (CBC) together with CBP20. CBC has been reported to mediate the stimulatory functions of the cap in mRNA processing, 3'-end formation, and U snRNA export (36). E7070 and ER-68487 also repressed significantly the expression of *cleavage stimulation factor*, *SRp55*, *KOC*, *eIF2B ϵ* , and *ribosomal protein S6 kinase 2*. These genes are known to be involved in either mRNA processing or translation. In this regard, cellular pathways sensitive to compounds of the E7070 sort may be connected with the regulatory mechanism of mRNA biogenesis.

(b) Phospholipid scramblase 1 has been shown to cause a bidirectional movement of plasma membrane phospholipids by an increase in intracellular calcium (37). With reference to this down-regulation, several [Ca²⁺]_i-responsive genes, including *calcineurin A1*, *CaM kinase II*, and *tropomyosin*, were decreased in their expression >2-fold in both E7070- and ER-68487-treated HCT116-C9 cells. These findings imply a potential link between intracellular

calcium signaling and biological activity of the E7070 class. Finally, the precise role of PDCD2 is still unknown, although its rat homologue Rp8 is thought to be associated with programmed cell death (38).

Further intensive work to identify a primary molecular target(s) of E7070 is currently under way and will be reported in due course, hopefully clarifying the relevance between functions of the target(s) and all of the cellular responses discussed above. We herein demonstrate an integrated strategy for the discovery and development of novel anticancer drugs, consisting of sulfonamide-focused compound libraries, phenotypic antitumor screens, and array-based transcriptional profiling. The present study includes a translational research that may be informative in relation to potential pharmacodynamic end points for assessing the E7010 and E7070 classes of sulfonamide antitumor agents.

References

- Schreiber, S. L. Target-oriented and diversity-oriented organic synthesis in drug discovery. *Science (Wash. DC)*, 287: 1964–1969, 2000.
- Drews, J. Drug discovery: a historical perspective. *Science (Wash. DC)*, 287: 1960–1964, 2000.
- Maren, T. H. Relations between structure and biological activity of sulfonamides. *Ann. Rev. Pharmacol. Toxicol.*, 16: 309–327, 1976.
- Supuran, C. T., and Scozzafava, A. Carbonic anhydrase inhibitors and their therapeutic potential. *Exp. Opin. Ther. Patents*, 10: 575–600, 2000.
- Yoshino, H., Ueda, N., Nijima, J., Sugumi, H., Kotake, Y., Koyanagi, N., Yoshimatsu, K., Asada, M., Watanabe, T., Nagasu, T., Tsukahara, K., Iijima, A., and Kitoh, K. Novel sulfonamides as potential, systemically active antitumor agents. *J. Med. Chem.*, 35: 2496–2497, 1992.
- Owa, T., Yoshino, H., Okauchi, T., Yoshimatsu, K., Ozawa, Y., Sugi, N. H., Nagasu, T., Koyanagi, N., and Kitoh, K. Discovery of novel antitumor sulfonamides targeting G1 phase of the cell cycle. *J. Med. Chem.*, 42: 3789–3799, 1999.
- Owa, T., Okauchi, T., Yoshimatsu, K., Sugi, N. H., Ozawa, Y., Nagasu, T., Koyanagi, N., Okabe, T., Kitoh, K., and Yoshino, H. A focused compound library of novel *N*-(7-indolyl)benzenesulfonamides for the discovery of potent cell cycle inhibitors. *Bioorg. Med. Chem. Lett.*, 10: 1223–1226, 2000.
- Owa, T., and Nagasu, T. Novel sulphonamide derivatives for the treatment of cancer. *Exp. Opin. Ther. Patents*, 10: 1725–1740, 2000.
- Yoshimatsu, K., Yamaguchi, A., Yoshino, H., Koyanagi, N., and Kitoh, K. Mechanism of action of E7010: inhibition of mitosis by binding to the colchicine site of tubulin. *Cancer Res.*, 57: 3208–3213, 1997.
- Koyanagi, N., Nagasu, T., Fujita, F., Watanabe, T., Tsukahara, K., Funahashi, Y., Fujita, M., Taguchi, T., Yoshino, H., and Kitoh, K. *In vivo* tumor growth inhibition produced by a novel sulfonamide, E7010, against rodent and human tumors. *Cancer Res.*, 54: 1702–1706, 1994.
- Yamamoto, K., Noda, K., Yoshimura, A., Fukuoka, M., Furuse, K., and Niitani, H. Phase I study of E7010. *Cancer Chemother. Pharmacol.*, 42: 127–134, 1998.
- Ozawa, Y., Sugi, N. H., Nagasu, T., Owa, T., Watanabe, T., Koyanagi, N., Yoshino, H., Kitoh, K., and Yoshimatsu, K. E7070, a novel sulfonamide agent with potent antitumor activity *in vitro* and *in vivo*. *Eur. J. Cancer*, 37: 2275–2282, 2001.
- Punt, C. J., Fumoleau, P., van de Walle, B., Faber, M. N., Ravic, M., and Campone, M. Phase I and pharmacokinetic study of E7070, a novel sulfonamide, given at a daily times five schedule in patients with solid tumors. A study by the EORTC-early clinical studies group (ECSG). *Ann. Oncol.*, 12: 1289–1293, 2001.
- Punt, C. J. A., Fumoleau, P., Walle, B. V. D., Deporte-Fety, R., Bourcier, C., Faber, M., Ravic, M., and T. Wagener, D. J. *Proc. Am. Assoc. Cancer Res.*, 41: 609, 2000.
- Raymond, E., ten Bokkel-Huinink, W. W., Taieb, J., Beijnen, J. H., Mekhaldi, S., Kroon, K., Wanders, J., Ravic, M., Fumoleau, P., Ducreux, M., Escudier, B., and Armand, J. P. *Proc. Am. Assoc. Cancer Res.*, 41: 611, 2000.
- Schena, M., Shalon, D., Davis, R. W., and Brown, P. O. Quantitative monitoring of gene expression patterns with a complementary DNA microarray. *Science (Wash. DC)*, 270: 467–470, 1995.
- Lockhart, D. J., Dong, H., Byrne, M. C., Follettie, M. T., Gallo, M. V., Chee, M. S., Mittmann, M., Wang, C., Kobayashi, M., Horton, H., and Brown, E. L. Expression monitoring by hybridization to high-density oligonucleotide arrays. *Nat. Biotechnol.*, 14: 1675–1680, 1996.
- Stockwell, B. R., Hardwick, J. S., Tong, J. K., and Schreiber, S. L. Chemical genetic and genomic approaches reveal a role for copper in specific gene activation. *J. Am. Chem. Soc.*, 121: 10662–10663, 1999.
- Marton, M. J., DeRisi, J. L., Bennett, H. A., Iyer, V. R., Meyer, M. R., Roberts, C. J., Stoughton, R., Burchard, J., Slade, D., Dai, H., Bassett, D. E., Jr., Hartwell, L. H., Brown, P. O., and Friend, S. H. Drug target validation and identification of secondary drug target effects using DNA microarrays. *Nat. Med.*, 4: 1293–1301, 1998.
- Hardwick, J. S., Kuruville, F. G., Tong, J. K., Shamji, A. F., and Schreiber, S. L. Rapamycin-modulated transcription defines the subset of nutrient-sensitive signaling pathways directly controlled by the Tor proteins. *Proc. Natl. Acad. Sci. USA*, 96: 14866–14870, 1999.
- Scherf, U., Ross, D. T., Waltham, M., Smith, L. H., Lee, J. K., Tanabe, L., Kohn, K. W., Reinhold, W. C., Myers, T. G., Andrews, D. T., Scudiero, D. A., Eisen, M. B., Sausville, E. A., Pommier, Y., Botstein, D., Brown, P. O., and Weinstein, J. N. A gene expression database for the molecular pharmacology of cancer. *Nat. Genet.*, 24: 236–244, 2000.
- Dittrich, C., Dumez, H., Calvert, H., Hanauske, A. R., Ravic, M., Faber, M., van Houten, T., Wanders, J., and Fumoleau, P. *Proc. Am. Assoc. Cancer Res.*, 41: 609, 2000.
- Mosmann, T. Rapid colorimetric assay for cellular growth and survival: application to proliferation and cytotoxicity assays. *J. Immunol. Methods*, 65: 55–63, 1983.
- Rödicker, F., Stiewe, T., Zimmermann, S., and Pützer, B. M. Therapeutic efficacy of E2F1 in pancreatic cancer correlates with *TP73* induction. *Cancer Res.*, 61: 7052–7055, 2001.
- Liu, X. M., Wang, L. G., Kreis, W., Budman, D. R., and Adams, L. M. Differential effect of vinorelbine versus paclitaxel on ERK2 kinase activity during apoptosis in MCF-7 cells. *Br. J. Cancer*, 85: 1403–1411, 2001.
- Kumar, R., and Korutla, L. Induction of expression of interferon-stimulated gene factor-3 (ISGF-3) proteins by interferons. *Exp. Cell Res.*, 216: 143–148, 1995.
- Hwang, L. H., and Murray, A. W. A novel yeast screen for mitotic arrest mutants identifies *DOC1*, a new gene involved in cyclin proteolysis. *Mol. Biol. Cell*, 8: 1877–1887, 1997.
- Rosania, G. R., Chang, Y.-T., Perez, O., Sutherland, D., Dong, H., Lockhart, D. J., and Schultz, P. G. Myoseverin, a microtubule-binding molecule with novel cellular effects. *Nat. Biotechnol.*, 18: 304–308, 2000.
- Ben-Ze'ev, A., Farmer, S. R., and Penman, S. Mechanisms of regulating tubulin synthesis in cultured mammalian cells. *Cell*, 17: 319–325, 1979.
- Chen, Y., McPhie, D. L., Hirschberg, J., and Neve, R. L. The amyloid precursor protein-binding protein APP-BP1 drives the cell cycle through the S-M checkpoint and causes apoptosis in neurons. *J. Biol. Chem.*, 275: 8929–8935, 2000.
- Nigg, E. A. Cyclin-dependent kinase 7: at the cross-roads of transcription, DNA repair and cell cycle control? *Curr. Opin. Cell Biol.*, 8: 312–317, 1996.
- Rossignol, M., Kolb-Cheynel, I., and Egly, J. M. Substrate specificity of the cdk-activating kinase (CAK) is altered upon association with TFIID. *EMBO J.*, 16: 1628–1637, 1997.

33. Yankulov, K. Y., and Bentley, D. L. Regulation of CDK7 substrate specificity by MAT1 and TFIIH. *EMBO J.*, *16*: 1638–1646, 1997.
34. Araujo, S. J., Tirode, F., Coin, F., Pospiech, H., Syvaaja, J. E., Stucki, M., Hubscher, U., Egly, J. M., and Wood, R. D. Nucleotide excision repair of DNA with recombinant human proteins: definition of the minimal set of factors, active forms of TFIIH, and modulation by CAK. *Genes Dev.*, *14*: 349–359, 2000.
35. Korn, E. L., Arbuck, S. G., Pluda, J. M., Simon, R., Kaplan, R. S., and Christian, M. C. Clinical trial designs for cytostatic agents: are new approaches needed? *J. Clin. Oncol.*, *19*: 265–272, 2001.
36. McKendrick, L., Thompson, E., Ferreira, J., Morley, S. J., and Lewis, J. D. Interaction of eukaryotic translation initiation factor 4G with the nuclear cap-binding complex provides a link between nuclear and cytoplasmic functions of the m(7) guanosine cap. *Mol. Cell. Biol.*, *21*: 3632–3641, 2001.
37. Basse, F., Stout, J. G., Sims, P. J., and Wiedmer, T. Isolation of an erythrocyte membrane protein that mediates Ca²⁺-dependent transbilayer movement of phospholipid. *J. Biol. Chem.*, *271*: 17205–17210, 1996.
38. Kawakami, T., Furukawa, Y., Sudo, K., Saito, H., Takami, S., Takahashi, E., and Nakamura, Y. Isolation and mapping of a human gene (PDCD2) that is highly homologous to *Rp8*, a rat gene associated with programmed cell death. *Cytogenet. Cell Genet.*, *71*: 41–43, 1995.

Molecular Cancer Therapeutics

Profiling Novel Sulfonamide Antitumor Agents with Cell-based Phenotypic Screens and Array-based Gene Expression Analysis

Akira Yokoi, Junro Kuromitsu, Takatoshi Kawai, et al.

Mol Cancer Ther 2002;1:275-286.

Updated version Access the most recent version of this article at:
<http://mct.aacrjournals.org/content/1/4/275>

Cited articles This article cites 34 articles, 15 of which you can access for free at:
<http://mct.aacrjournals.org/content/1/4/275.full#ref-list-1>

Citing articles This article has been cited by 2 HighWire-hosted articles. Access the articles at:
<http://mct.aacrjournals.org/content/1/4/275.full#related-urls>

E-mail alerts [Sign up to receive free email-alerts](#) related to this article or journal.

Reprints and Subscriptions To order reprints of this article or to subscribe to the journal, contact the AACR Publications Department at pubs@aacr.org.

Permissions To request permission to re-use all or part of this article, use this link
<http://mct.aacrjournals.org/content/1/4/275>.
Click on "Request Permissions" which will take you to the Copyright Clearance Center's (CCC) Rightslink site.